Journal of Ceramic Processing Research. Vol. 13, Special. 1, pp. s37~s41 (2012)

J O U R N A L O F
Ceramic Processing Research

Effect of SiO_2/B_2O_3 ratio on Li ion conductivity of a Li_2O-B_2O_3-SiO_2 glass electrolyte

Young Han Kim, Mi Young Yoon, Eun Jung Lee and Hae Jin Hwang*
Division of Materials Science and Engineering, Inha University, Incheon 402-751, Korea

A lithium ion conducting borosilicate glass was fabricated by a conventional melt quenching technique from a mixture of Li_2CO_3, B_2O_3 and SiO_2 powders. The Li ion conductivity of the lithium borosilicate glasses was evaluated in terms of the SiO_2/B_2O_3 ratio. In the Li_2O-B_2O_3-SiO_2 ternary glass, the glass forming region decreases with an increasing Li_2O content. At the same Li_2O, the crystallization tendency of the glass samples increases with the SiO_2/B_2O_3 ratio, resulting in a reduced glass forming region in the Li_2O-B_2O_3-SiO_2 ternary glass. The electrical conductivity moderately depends on the SiO_2/B_2O_3 ratio in the Li_2O-B_2O_3-SiO_2 ternary glass. The conductivity of the glasses slightly increases with the SiO_2/B_2O_3 ratio. The observed phenomenon can be explained by the modification of the glass structure as a function of the SiO_2 content.

Key words: Solid electrolytes, Li ion conductivity, Solid state batteries, Lithium boroslicate glasses.

Introduction

All solid state rechargeable thin film Li-ion batteries have received much interest due to their potential application in microdevices, which are potential candidates as a power source for small electronic products, such as semiconductor diagnostic wafers, smart cards, sensors and radio frequency identification tags, and medical products, such as pacemakers and other implantable surgical devices. Li-ion conducting solid electrolytes is the key materials for the solid-state thin film batteries. The lithium ion conducting solid electrolyte should be highly conductive, compatible with electrode materials, such as lithium metal, and chemically stable in an air atmosphere. In addition, it should be easily fabricated at low temperatures via thin film fabrication processes such as sputtering.

Lithium lanthanum titanate [1-2], NASICON-[3], NISICON-[4-5] and garnet-[6] type Li ion conductors are typical crystalline lithium ion conductors, while oxide or sulfide glasses are amorphous Li ion conductors. Although the crystalline lithium ion conductors show high conductivities of up to 10^{-3} to 10^{-4} Scm^{-1}, they can be realized only by making a sample of a single crystalline form. In addition, some materials are not phase-compatible with Li metal due to the reduction of the transition metal ion, such as Ti^{4+}.

Amorphous-type Li-ion conductors offer several advantages over crystalline conductors, such as low temperature processing and isotropic conductivity. At present, lithium phosphorous oxynitride (LiPON) glass with a typical composition of $Li_{2.88}PO_{3.73}N_{0.14}$ has been most widely used for the all solid-state thin film batteries [7]. LiPON is prepared by the sputtering technique using a Li_3PO_4 target in an N_2 atmosphere. The incorporation of nitrogen into lithium phosphate allows LiPON to be chemically stable with Li metal and not to decompose even at 5 V. However, the problems of its poor reproducibility and structural degradation in an air atmosphere remain unsolved [8].

On the other hand, lithium alumino-, boro-, and phosphor- silicates have been systematically studied for their excellent chemical and thermal stability [9-11]. However, the unsatisfactorily poor lithium ion conductivity, about 10^{-7} to 10^{-8} Scm^{-1} at room temperature, severely limits the potential use for the lithium ion electrolyte. In this study, lithium borosilicate (Li_2O-B_2O_3-SiO_2) glasses with 40, 45 and 47.5 mol% of Li_2O were fabricated by the melt quenching method. The lithium ion conductivities of the glasses were measured at the temperature range from room temperature to 200 °C using an ac impedance analyzer and are discussed in terms of the SiO_2/B_2O_3 ratio in the Li_2O-B_2O_3-SiO_2 composition.

Experimental Procedure

Lithium carbonate (Li_2CO_3), boron oxide (B_2O_3) and silica (SiO_2) were used as the starting materials. Appropriate amounts of the starting materials were mixed well and heated at 1000~1200 °C for 3 hours in a platinum crucible. A homogeneous free flowing melt was obtained at these temperatures, which was then quenched in a graphite mold. The bar-shaped glass sample (20×20×100 mm) was then annealed at 400~500 °C for

*Corresponding author:
Tel : +82-32-860-7521
Fax: +82-32-862-4482
E-mail: hjhwang@inha.ac.kr

subsequent machining.

X-ray diffraction (XRD) analysis were performed using a diffractometer (DMAX-2500, Rigaku, Japan) to confirm the crystallization of the sample. Differential thermal analysis (DTA) was carried out to determine glass transition temperature using a TG-DTA instrument (Diamond TG/DTA, Perkin Elmer, USA). A Fourier transform infrared (FT-IR) spectrometer (FTS-165, Bio-Rad, USA) and a Raman spectrometer (RFS 100/S, Bruker Optics Inc., Germany) were used to confirm the network structure of the glass samples in the wave number range of 400 to 1800 cm^{-1}.

Li ion conductivity measurements were performed in the range from room temperature to 200 °C by an ac impedance analyzer (IM6, Zahner Co., Germany) in the frequency range of 1 Hz-1 MHz. A disk-type sample (20×20×0.25 mm) was cut from the bar-shaped glass and polished using a # 2000 SiC paper. Platinum ionic blocking electrodes with an area of 1 cm^2 were deposited by sputtering (E-1030, Hitachi Co. Ltd., Japan) on both sides of the sample.

Results and Discussion

Fig. 1 shows the typical XRD patterns of the lithium borosilicate glasses with the compositions of $40Li_2O$-$(60-x)B_2O_3$-$xSiO_2$ and $45Li_2O$-$(55-x)B_2O_3$-$xSiO_2$. There was no characteristic peak that corresponded to any crystalline phase, implying that the obtained samples are all glass phase. The glass forming region in the Li_2O-B_2O_3-SiO_2 composition diagram is shown in Fig. 2. The open circles denote the compositions for which glassy and transparent samples were obtained, and the closed circles indicate the samples that contain a small amount of crystallites. At Li_2O = 47.5 mol%, the glass formation region is narrow, while it increased with a decreasing Li_2O content. For $47.5Li_2O$-$(52.5-x)B_2O_3$-$xSiO_2$, the samples with more than 30 mol% and less than 10 mol% of SiO_2 were partially crystallized, while all the samples containing 40 mol% Li_2O were glassy.

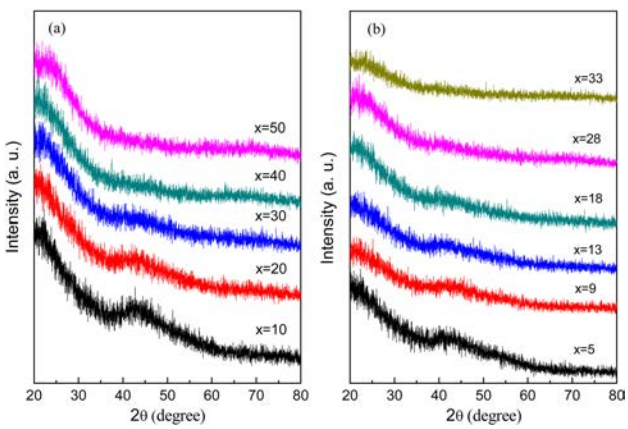

Fig. 1. XRD patterns of $40Li_2O$-$(60-x)B_2O_3$-$xSiO_2$ (a) and $45Li_2O$-$(55-x)B_2O_3$-$xSiO_2$ (a) glasses.

Tatsumisago et al. reported that the limit of glass formation in the Li_2O-SiO_2 system is 40 mol% Li_2O in the case of the normal melt quenching technique [12]. Maia et al. fabricated lithium borosilicate glasses with 40 mol% Li_2O by melt quenching [13]. Therefore, the observed result appears to be reasonable.

As the Li_2O content increases, the glass forming region gradually shrinks to compositions with less SiO_2 content, indicating that Li_2O increases the crystallization tendency in the Li_2O-B_2O_3-SiO_2 system. For the samples with the same Li_2O mol%, the sample with a higher molar content of B_2O_3 was glassy. This phenomenon is believed partly by the lower melting temperature of the Li_2O-B_2O_3 glass than that of the Li_2O-SiO_2 glass [13]. In addition, B_2O_3 can decrease the viscosity and crystallization tendency of Li_2O-SiO_2 glasses, resulting in a wider glass formation region. However, the glass forming region shrank with a

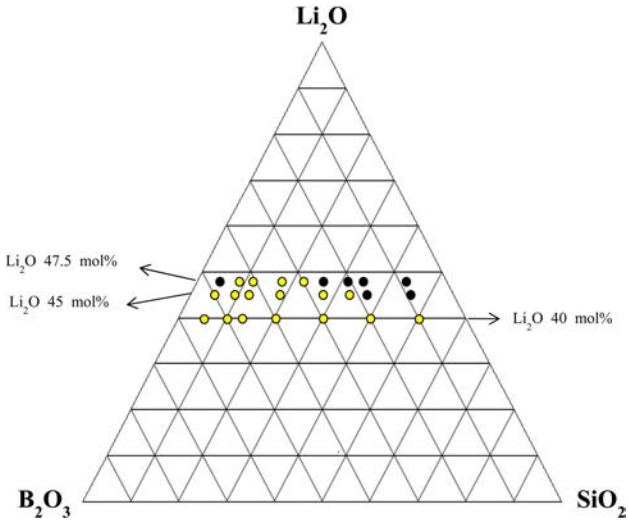

Fig. 2. Glass forming region of Li_2O-B_2O_3-SiO_2 glasses in this study. The gray and closed circles indicate the perfect transparent glass and partially crystallized glass, respectively.

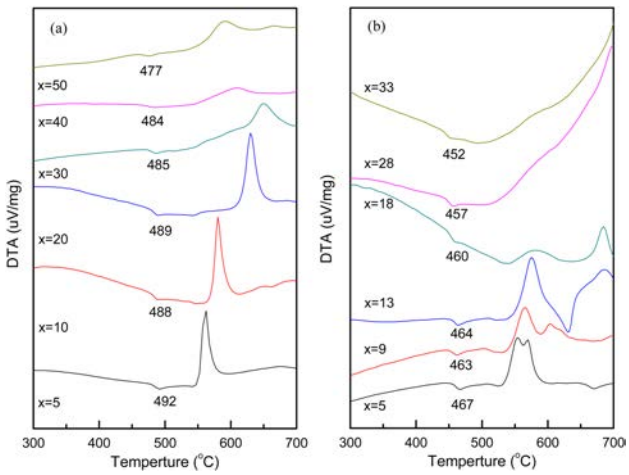

Fig. 3. DTA curves of $40Li_2O$-$(60-x)B_2O_3$-$xSiO_2$ (a) and $45Li_2O$-$(55-x)B_2O_3$-$xSiO_2$ (b) glasses. the heating rate was 10 °C/min.

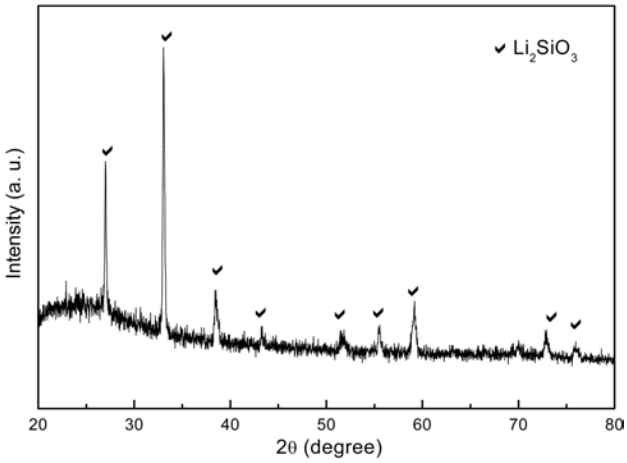

Fig. 4. XRD pattern of the $45Li_2O$-$18B_2O_3$-$37SiO_2$ glass.

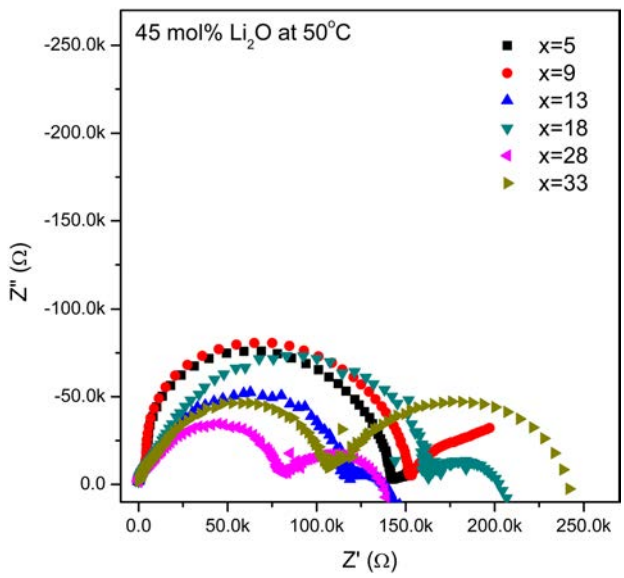

Fig. 5. Impedance spectra of $45Li_2O$-$(55\text{-}x)B_2O_3$-$xSiO_2$ glasses at 50 °C

further substitution of SiO_2 by B_2O_3. The glass with 47.5 mol% Li_2O and the $SiO_2/B_2O_3 = 0.9$ was found to be partially crystallized.

Fig. 3 shows the DTA curve for the $40Li_2O$-$(60\text{-}x)B_2O_3$-$xSiO_2$ and $45Li_2O$-$(55\text{-}x)B_2O_3$-$xSiO_2$ glasses as a function of the SiO_2 content. The small endothermic peak appears between 450 and 500 °C, followed by a large exothermic peak between 540 and 650 °C. Each peak is attributed to the glass transition temperature and crystallization temperature, respectively. The glass transition temperature tends to decrease with an increase in the SiO_2 content for the two systems, suggesting that the glasses with a higher SiO_2 content have an open structure and therefore a higher ionic conductivity. On the other hand, the crystallization temperature increases with an increasing SiO_2 content in the glass composition. This phenomenon is well consistent with the narrow glass formation region observed in the $45Li_2O$-$(55\text{-}x)B_2O_3$-$xSiO_2$ glass system.

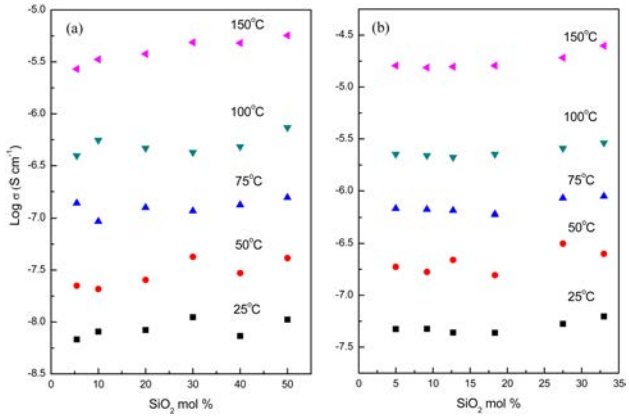

Fig. 6. Conductivity of the $40Li_2O$-$(60\text{-}x)B_2O_3$-$xSiO_2$ (a) and $45Li_2O$-$(55\text{-}x)B_2O_3$-$xSiO_2$ (b) glasses at various temperatures as a function of SiO_2 mole fraction.

Fig. 4 shows the XRD pattern for the sample with the composition of $45Li_2O$-$18B_2O_3$-$37SiO_2$. It was found that all peaks are attributed to the Li_2SiO_3.

Fig. 5 shows the impedance spectra, measured at 50 °C, for the Pt/glass electrolyte with 45 mol% Li_2O/Pt cells. All of the samples exhibited the typical impedance spectrum observed in the case of cells consisting of a glass electrolyte and blocking electrodes, such as Pt, i.e., one semicircle in the high and medium frequency range, followed by a straight line due to the polarization or diffusion of Li ions at the interface between the glass electrolyte and Pt blocking electrode [14]. The bulk resistance of the glass electrolyte can be obtained from the right intercept of the semicircle with the real axis (x axis) and the conductivity is then calculated from the resistance, thickness of the electrolyte and area of the electrode.

Fig. 6 presents the log conductivity for the $40Li_2O$-$(60\text{-}x)B_2O_3$-$xSiO_2$ and $45Li_2O$-$(55\text{-}x)B_2O_3$-$xSiO_2$ glass electrolyte as a function of the SiO_2 content. The glass samples containing more Li_2O showed higher conductivity. This phenomenon can be explained by the increase in the Li ion concentration of the glass and the accompanying change in the chemical bonding of the glass structure, which is the increased number of non-bridging oxygens(NBOs) [15-16]. In addition, the conductivity increased with an increasing SiO_2 content, suggesting that the mixed former effect is responsible for the high conductivity observed in the ternary glass. For a lithium borate binary glass, adding SiO_2 as the second glass former can allow the borate glass to be more de-polymerized, because SiO_2 can play the role of a network modifier, resulting in an increased ortho-borate or pyro-borate content, which can enhance the conductivity in the ternary glass with a small amount of SiO_2 [16].

Fig.7 shows the Raman spectra of the $40Li_2O$-$(60\text{-}x)B_2O_3$-$xSiO_2$ and $45Li_2O$-$(55\text{-}x)B_2O_3$-$xSiO_2$ glass samples. The peaks at 780 cm^{-1} are due to the trigonal deformation of borate rings with BO_4 units such as di-, tri- and tetra-borate, whereas the peak at 960 cm^{-1} is

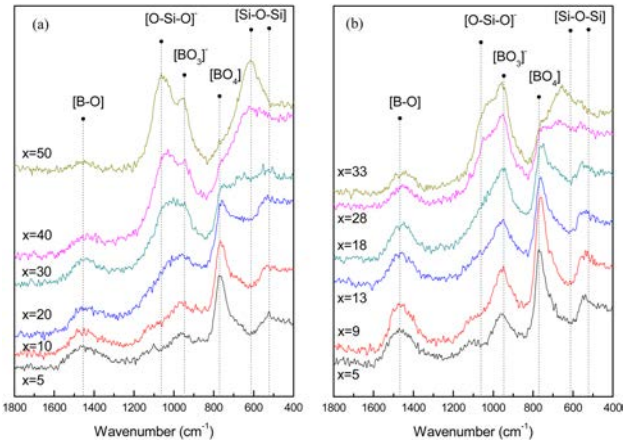

Fig. 7. Raman spectra of $40Li_2O$-(60-x)B_2O_3-xSiO_2 (a) and $45Li_2O$-(55-x)B_2O_3-xSiO_2 (b) glasses.

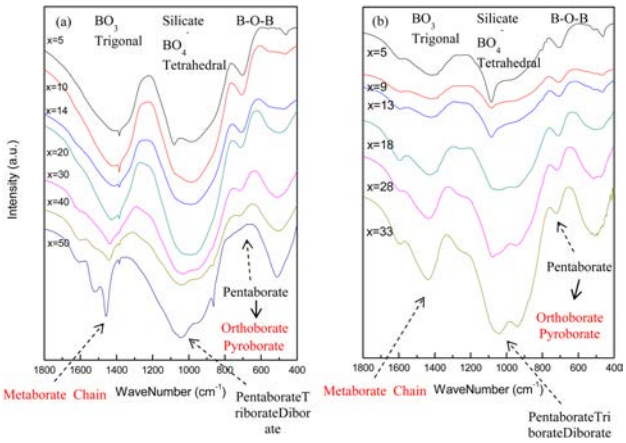

Fig. 8. FT-IR spectra of $40Li_2O$-(60-x)B_2O_3-xSiO_2 (a) and $45Li_2O$-(55-x)B_2O_3-xSiO_2 (b) glasses.

due to the stretching of the B-nonbridging oxygen of pyroborate ($[BO_3]^-$). The band between 1400 and 1550 cm^{-1} is associated with the stretching vibrations of the B-O bonds in the BO_3 units. On the other hand, the peaks which are associated with the SiO_2 network were observed in two frequency regions, 500-700 cm^{-1} and 900-1100 cm^{-1}. The band between 500 and 700 cm^{-1} are assigned to bridging Si-O-Si vibration, while the peak at 1060 cm^{-1} is attributed to the non-bridging Si-O stretching mode of SiO_4 unit. Fig. 7 suggests that as the SiO_2 content increases, the $[BO_4]$ structure disappears and at the same time, the non-bridging $[BO_3]^-$ and $[SiO_4]^{-1}$ structures gradually increase.

Fig. 8 shows FT-IR spectra of the $40Li_2O$-(60-x)B_2O_3-xSiO_2 and $45Li_2O$-(55-x)B_2O_3-xSiO_2 glass samples. The band between 1400 and 1460 cm^{-1} is attributed to the non-bridging oxygen of trigonal BO_3 in metaborate, pyroborate and othoborate. This vibration band is clearly observed in the glass samples containing more than 30% of SiO_2 and its intensity increases with an increasing SiO_2 content, which results in enhanced ionic conductivity as a function of SiO_2. The band at 1385 cm^{-1} is assigned to the B-O-B stretching vibration which results from the condensation of BO_3, suggesting the formation of diborate from pentaborate. The appearance of this band indicates the existence of the bridging oxygen in the glass sample.

The broad band at 1080-1040 cm^{-1} is associated with the vibration of Si-O-Si and Si-O-B bonds observed in borate and borosilicate glasses. In addition, the band at 1080 cm^{-1} may be due to the tetragonal BO_4^- and the decrease in the band intensity is related to the disappearance of pentaborate, diborate and triborate, which have the bridging oxygen in the structure[17]. The bands at 707 cm^{-1} observed in x = 5 may be due to the vibration band in the B-O boroxyl ring. This band is shifted into the high frequency region and the intensity decreases with an increasing SiO_2 content. These phenomena might be responsible for the glass structure change from the pentaborate with bridging oxygen to pyroborate and orthoborate with non-bridging oxygen.

Conclusion

A lithium borosilicate glass, Li_2O-B_2O_3-SiO_2, was fabricated by the conventional melt quenching technique. The glass forming region shrank as the Li_2O content increased, while B_2O_3 decreased the viscosity and crystallization tendency of the Li_2O-SiO_2 glass, resulting in the wider glass formation domain. The glass transition temperature decreased with an increasing SiO_2 content, which means that the SiO_2-rich lithium borosilicate glass has a more open structure. The lithium ion conductivity of the glasses increased with an increasing SiO_2 content, although the increase was modest. This enhanced conductivity might be associated with the increase in the non-bridging oxygen and the resulting improved lithium ion mobility.

Acknowledgements

This work was supported by the Korea Research Foundation Grant funded by the Korean Government (MOEHRD, Basic Research Promotion Fund) (KRF-2008-521-D00186). A part of this work was supported by the National Research Foundation of Korea (NRF) grant funded by the Korea government (MEST) (No. 2011-0015512).

References

1. G.Y. Adachi, N. Imanaka, H. Aono, Adv. Mater. 8 (1996) 127.
2. S. Stramare, V. Thangadurai, and W. Weppner, Chem. Mater. 15 (2003) 3974.
3. H. Aono, E. Sugimoto, Y. Sadaoka, N. Imanaka, G. Adachi, J. Electrochem. Soc. 136 (1989) 590.
4. A.D. Robertson, A.W. West, A.G. Ritchie, Solid State Ionics 104 (1997) 1.
5. M. Murayama, R. Kanno, M. Irie, S. Ito, T. Hata, N.

Sonoyama, Y. Kawamoto, J. Solid State Chem. 168 (2002) 140.
6. V. Thangadurai, H. Kaack, and W.J.F. Weppner, J. Am. Ceram. Soc. 86 (2004) 437.
7. X. Yu, J.B. Bates, G.E. Jellison, F.X. Hart, J. Electrochem. Soc. 144 (1997) 524.
8. P. Birke, W.F. Chu, W. Weppner, Solid State Ionics 93 (1997) 1.
9. J. Rogez, P. Knauth, A. Garnier, H. Ghobarkar, O. Schaf, J. Non-Crystalline Solids 262 (2000) 177.
10. P. Kluva´nek, R. Klement, M. Karacon, J. Non-Cryst. Solids353 (2007) 2004.
11. M. Tatsumisago, K. Yoneo, N. Machida, T. Minami, J. Non-Cryst. Solids 95 (1987) 857.
12. M. Tatsumisago and T. Minami, Mater. Chem. Phys. 18 (1987) 1.
13. L.F. Maia, A.C.M. Rodrigues, Solid State Ionics 168 (2004) 87.
14. X. Qian, N. Gu, Z. Cheng, X. Yang, E. Wang, S. Dong, Electrochim.Acta 46 (2001) 1829.
15. C.-H. Lee, K.H. Joo, J.H. Kim, S.G. Woo, H.-J. Sohn, T. Kang, Y. Park, J.Y. Oh, Solid State Ionics 149 (2002) 59.
16. S.H. Lee, K.I. Cho, J.B. Choi, D.W. Shin, J. Power Sources 162 (2006) 1341.
17. P. Muralidharan, M. Venkateswarlu, N. Satyanarayana, Solid State Ionics, 166 (2004) 27.